Clinical and Applied Thrombosis/Hemostasis
2018, Vol. 24(9S) 104S-116S

DOI: 10.1177/1076029618792304
journals.sagepub.com/home/cat
SAGE

Glucose Concentration Affects Fibrin Clot Structure and Morphology as Evidenced by Fluorescence Imaging and Molecular Simulations

Jacob E. Hood, BS, MS[1], Sumith Yesudasan, BS, MS, PhD[1], and Rodney D. Averett, BS, MS, PhD[1]

Abstract

Although in vivo studies have been conducted in the past to determine hyperglycemic effects and influence on clotting risk in patients with diabetes, the true extent of hyperglycemia on unstable and spontaneous clot formation remains highly debated. Factors such as increased glycation, elevated fibrinogen concentration, elevated prothrombin levels, and decreased plasminogen are known to influence fibrin conversion, clot morphology, and thrombus formation in these individuals. In this regard, the isolated effects of hyperglycemia on irregular fibrin clot formation were investigated in a controlled fibrinogen system. In this study, fibrin clot characteristic differences at 3 glucose concentrations were analyzed to determine the effects of glucose concentration on fibrinogen glycation and fibrin clot morphology using confocal microscopy, glycation quantification, molecular simulations, and image processing methods. Algorithms coupled with statistical analysis support in vivo findings that hyperglycemia increases fibrinogen glycation, with ensuing altered fibrin clot structure characteristics. Our experimental and molecular simulation results consistently show an increased glucose adsorption by fibrinogen with increased glucose concentration. Significant differences in clot structure characteristics were observed, and the results of this work can be used to further develop diagnostic tools for evaluating clotting risk in individuals with hypercoagulable and hyperglycemic conditions.

Keywords

fibrin, glycated fibrinogen, morphology, molecular dynamics, clot structure, diabetes

Introduction

From a molecular perspective, thrombus and fibrin formation is regulated by the precursor molecule fibrinogen.[1] Fibrinogen, a 340-kDa, 46-nm-long glycoprotein, is comprised of 2 three-paired Aα, Bβ, and γ polypeptide chains (ie, D-regions) and a central E-region that are linked together through 29 disulfide bonds.[2] As 4 separate disulfide bonds are dissolved, fibrinogen is converted into fibrin through thrombin-catalyzed removal of fibrinopeptides A and B (FpA and FpB) from the N-terminal ends of a single fibrinogen molecule. Removal of FpA and FpB exposes a terminal disulfide knot (N-terminal disulfide knot, NDSK) and signifies the conversion of a single fibrinogen molecule into a fibrin monomer.[1-3] As fibrin monomers accumulate, 600- to 800-nm protofibrils form by repetitive binding of D and exposed NDSK regions in a 23 nm half-staggered fashion.[4] Subsequently, protofibrils grow into fibrin fibers, approximately ~100 nm in diameter, through lateral αC-region interactions.[4-8] Formed fibrin fibers further interact laterally and longitudinally to develop into the 3-dimensional structure of a fibrin matrix, which indicates the end of thrombus formation.[4-8] Fibrin conversion is important because it governs clot integrity and stability, and the thrombus is maintained structurally by the fibrin fibers that form during this process.[9] Therefore, as fibrin fibers determine how a thrombus will respond to stresses (eg, fibrinolytic behavior), studying fibrin fiber characteristics may explain clot etiology and the increased occurrence of spontaneous and unstable thrombi development, in particular hypercoagulable states.[10]

[1] School of Chemical, Materials, and Biomedical Engineering, College of Engineering, University of Georgia, Athens, GA, USA

Corresponding Author:
Rodney D. Averett, School of Chemical, Materials, and Biomedical Engineering, College of Engineering, University of Georgia, 597 D.W. Brooks Drive, Athens, GA 30602, USA.
Email: raverett@uga.edu

One condition that meets the criteria of a hypercoagulable state is diabetes mellitus (DM), as cardiovascular events have shown to be 37.2% higher in these patients.[11,12] Despite specific links to arterial cardiovascular disease, acute myocardial infarction, stroke, venous thromboembolism, and atherosclerosis, increased macrovascular complications in DM cannot be completely explained by typical cardiovascular risk factors.[11-16] Clinical studies have compared diabetic and native clot characteristics in an attempt to explain and reduce diabetic clot morbidity and mortality; however, DM clotting in patients remains a serious epidemiological concern.[11,17,18] In these clinical examinations, the defining characteristic of DM, resting hyperglycemia, is often used to justify changed fiber characteristics, clot stability, and thrombus behavior. However, the true extent of hyperglycemic influence on unstable and spontaneous clot formation in patients with DM remains highly debated. Factors such as hyperfibrinogenemia, hyperinsulinemia, dyslipidemia, hypertension, obesity, decreased fibrinolysis, endothelial dysfunction, and changed platelet aggregability are known to influence thrombus formation in these individuals.[11,14-16,19-24] For example, fibrinogen concentration is an established independent risk factor for cardiovascular disease, regardless of vascular event history.[25-29] Additionally, in animal studies, it is known that hyperfibrinogenemic mice exhibit changed fibrin fiber characteristics, quicker vessel occlusion, increased fibrin mass, and poor fibrinolytic behavior when compared to nonhyperfibrinogenemic controls.[30] As fibrinogen concentration is consistently higher in patients with diabetes, the true effects of hyperglycemia on fibrin conversion, fibrin fiber formation, clot stability, and thrombus behavior cannot be examined in vivo without first understanding hyperglycemic influences in vitro at a constant fibrinogen concentration.[25]

Although the true effects of hyperglycemia on fibrin conversion, fibrin fiber formation, clot stability, and thrombus behavior remain unclear, clinical studies still provide valuable comparisons of diabetic and controlled clot features that could be confirmed through in vitro experimentation. First, when compared to patients without diabetes, characteristics of fibrin clots from patients with diabetes are measurably denser, more rigid, less permeable, and contain thinner fiber diameters. Clots with these characteristics also demonstrate increased resistance to lysis, which could explain the increased incidence of macrovascular conditions.[31-35] An equilibrium of clotting and lysis conditions must be maintained to ensure hemostasis is efficient but does not cause thrombosis.[10,36] Additionally, increased fibrinogen glycation studies have been conducted in vivo to determine changes in clot characteristics and explain how these hyperglycemic influences increase cardiovascular risk.[16,37-39] Contrary to enzymatic glycosylation, which is highly regulated and integral to cellular function, nonenzymatic glycation is a spontaneous process of metabolism that may actually degrade the functionality of fibrinogen. In addition, this nonenzymatic glycation can alter fibrin conversion and cause a prothrombotic shift in hemostasis.[15,40] Glycemic control (HbA_{1c} reduction >0.5%) has been shown to improve fibrinogen glycation, rate of lateral aggregation, clot permeability, and lysis rate and significantly decrease thrombotic incidence in diabetic patients.[20,25,26,39,41-44] Although these research efforts support evidence that hyperglycemic influence contributes to altered fibrin clot characteristics, fibrinogen glycation has not been examined at a controlled fibrinogen concentration to confirm that hyperglycemia causes the increased glycated fibrinogen measurements. Some controlled experiments have been conducted to examine the isolated effects of hyperglycemia on fibrin clot characteristics in vitro; however, fibrinogen glycation was not quantified in these studies.[45,46] A combination of factors is known to influence fibrin conversion, fibrin–fiber formation and thrombus behavior. This study aims to examine the effects of hyperglycemia on fibrin clot characteristics in vitro and quantify glycated fibrinogen in a controlled fibrinogen system. In addition, we conducted molecular docking and molecular dynamics (MD) simulations to examine how glucose binding (ie, fibrinogen glycation) may influence fibrin clot characteristics in glycated fibrin structures.

Methods

The methods used in this research were (1) detection of fibrin clot characteristics at 3 glucose concentrations, (2) quantification of fibrinogen glycation, and (3) molecular docking and MD simulations to investigate glucose adsorption on the fibrinogen molecule.

Material Preparation

For the 3 glucose conditions (0.0, 6.0, and 10.0 mmol/L), equal concentrations of Plasminogen, von Willebrand Factor and fibronectin depleted fibrinogen (FIB 3) (ERL, Southbend, Indiana) and fibrinogen from human plasma, Alexa Fluor 488 conjugate (Fisher Scientific, Pittsburg, Pennsylvania) were integrated into 100-μL volumes. The 3 incubation conditions contained 6.8 g/L fibrinogen, 100 mmol/L NaCl, and specified amounts of glucose. A 10% solution of fibrinogen from human plasma, Alexa Fluor 488 conjugate was applied to working volumes as conducted in previous imaging studies of fibrin gels.[45,46] A 40 mmol/L stock glucose solution (TGDI) was prepared from D-glucose and deionized water, diluted with 50 mmol/L Tris buffer (Lonza, Basel, Switzerland), and stored at 4°C prior to use. For each glucose condition, 30 μL of TGDI was further diluted with 50 mmol/L Tris buffer to meet specified concentrations of glucose (20.0 and 33.3 mmol/L) for glucose (6.0 or 10.0 mmol/L) conditions. For the 0.0 mmol/L glucose condition, 30 μL of 50 mmol/L Tris buffer was used in lieu of TGDI to maintain consistent total incubation volumes for the 3 incubation conditions. Two μL of 5 mol/L NaCl was also included in each 100 μL volume to meet a physiological sodium concentration during incubation.[47] Volumes of materials required to meet the specified incubation conditions were mixed in 1.5-mL centrifuge tubes and incubated at 37°C in a 5L Isotemp Water Bath (Fisher Scientific) for 48 hours. During incubation, we used 6.8 mg/mL fibrinogen, 100 mmol/L NaCl

and varied the glucose concentration. For clot preparation, the thrombin solution was prepared from human α-thrombin (ERL, Southbend, Indiana), 1 mol/L $CaCl_2$, and 50 mmol/L Tris buffer. Stock human α-thrombin was diluted to 100 U/mL with 50 mmol/L Tris buffer and stored at −20°C prior to use. For these in vitro experiments, we selected glucose concentrations to represent unglycated and baseline conditions (0 mmol/L glucose), an elevated glucose concentration representative of patients with uncontrolled diabetes (6 mmol/L), and severely uncontrolled glycation in patients with diabetes (10 mmol/L).

Clot Polymerization

For imaging of fibrin clot structures, lifted platforms were prepared by affixing an adhesive (Scotch, 3 M, Minneapolis, Minnesota) 20 mm apart on sterile glass microscope slides. This adhesive was used to create each side of the platform and the space between the 2 sides was used to polymerize fibrin clots. For clot polymerization, 20 μL of an incubated fibrinogen solution and 20 μL of the prepared human μ-thrombin solution (1:1 dilution) was added to a clean 1.5 mL centrifuge tube and pipette mixed several times to homogenize the samples. From the resulting 40 μL solution, 30 μL of homogenized solution was immediately transferred to the sample loading area and allowed to polymerize for 2 hours prior to imaging, resulting in final concentrations of 3.4 mg/mL of fibrinogen, 0.5 U/mL human α-thrombin, and specified amounts of glucose. Five minutes after transferring the polymerized solution to the microscope slide, a 22 mm^2 transparent sterile cover slip was placed over the sample to seal the sample loading area and limit air exposure. This was also done to avoid contamination and to minimize dehydration during fibrin polymerization.

Confocal Laser Scanning Microscopy Imaging

Fibrin gels were imaged using a standard fluorescent confocal microscopy protocol on an laser scanning microscopy (LSM) 880 with 20× Plan-Apo/0.75 NA and DIC capability (Ziess, Oberkochen, Germany) at 2× zoom (512 × 512 pixels). A minimum of 9 *z* stacks was collected for each glucose condition with 3 representative areas collected from a single incubated fibrinogen solution. For each of the 9 *z* stacks of a glucose condition, a minimum of 60 *z* stack slices was collected at 0.5 μm vertical slices. For example, for the 0.0 mmol/L condition, *z* stacks were taken at 3 different locations on a particular fibrin sample, and this was repeated for a total of 3 times for this condition (0.0 mmol/L). Because there was a minimum of 60 slices per *z* stack, this resulted in a minimum number of images (N) of 540. This number of images provides a statistical equivalent representation of the fibrin samples investigated in this study for each glucose condition. This methodology was used to obtain representation of a glucose condition, variability within polymerized clots, and irregularity within a *z* stack for various fibrin clot samples.

Colorimetric Glucose Assay Procedure

A colorimetric glucose assay (Cayman Chemical, Ann Arbor, Michigan) was conducted on an EPOCH Microplate Spectrophotometer (BioTek, Winooski, Vermont) to quantify fibrinogen glycation. Sodium phosphate assay buffer (SPAB) at 1000 mg/dL glucose standard and lyophilized enzyme mixture were provided in the assay kit and prepared separately to perform the colorimetric glucose assay protocol. Sodium phosphate assay buffer was prepared by mixing the provided 10 mL of 250 mmol/L sodium phosphate with 40 mL of high performance liquid chromatography water. The enzyme mixture was prepared by reconstituting the provided lyophilized vial with 6 mL of the SPAB. A 100 mg/dL glucose standard was prepared by diluting the provided 1000 mg/dL glucose with SPAB. The standard curve was built by further diluting the 100 mg/dL glucose standard with SPAB (Supplemental Table 1) and performing the colorimetric assay.

The colorimetric assay protocol was conducted by adding 85 μL of SPAB, 15 μL of a homogenized standard, and 100 μL of colorimetric enzyme mixture to a well of a 96-well microplate, per instructions of the procedure. The 96-well microplate was incubated at 37°C for 10 minutes, and absorbance was measured at 510 nm. The protocol was repeated 2 times for each diluted homogenized standard, and the standard curve was built by fitting measured absorbance to known glucose concentrations.

The colorimetric glucose assay was conducted under the 3 glucose conditions (0.0 mmol/L, 6.0 mmol/L, and 10.0 mmol/L), containing 6.8 mg/mL FIB 3, 100 mmol/L NaCl, and diluted concentrations of a 40 mmol/L glucose stock buffer to correspond with appropriate conditions for LSM imaging. After preparing glucose conditions, a 1:4 dilution of solution to SPAB was in a 1.5-mL centrifuge tube, and the undiluted sample was placed in the 5 L Isotemp Water Bath and incubated at 37°C for 48 hours. The colorimetric glucose assay protocol was conducted under diluted glucose conditions by adding 15 μL of homogenized sample, 85 μL of SPAB, and 100 μL of colorimetric enzyme mixture to a well of a 96-well microplate. The microplate was incubated at 37°C for 10 minutes, and absorbance was read at 510 nm. Five samples per condition were measured, and 3 readings were recorded for each sample. This protocol was repeated under the undiluted glucose conditions after 48 hours of incubation, and the 0- and 48-hour absorbance readings were used in subsequent calculations. The change in free glucose over 48 hours was converted into a quantifiable measurement ($mol_{glucose}/mol_{fibrinogen}$) for the known concentration of fibrinogen.

Algorithms Used to Determine Fibrin Clot Characteristics

From fluorescence *z* stack images, feature detection algorithms were employed to determine fibrin clot structure characteristics. Specifically, we determined how glucose concentration affected fibrin fiber overlap, fibrin fiber length, fiber matrix porosity, and fractal dimension. Fibrin fiber overlap was

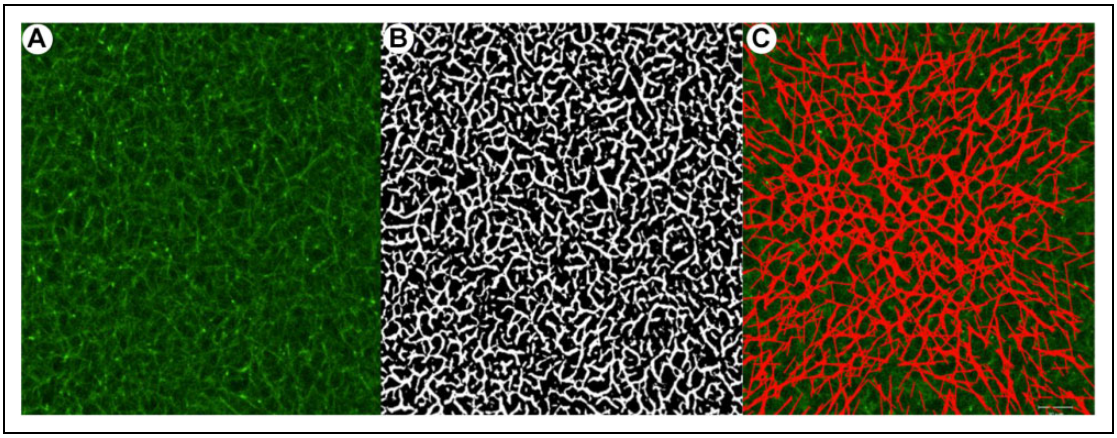

Figure 1. Image processing of a fluorescence fibrin fiber matrix using multiple feature detection techniques.

calculated by computing the number of overlaps (intersections) for each individually polymerized fibrin fiber. Fibrin fiber length was calculated by computing the length of each generated Hough line, and this fiber length was later converted from pixels into a quantifiable length measurement. Fiber matrix porosity was calculated by dividing the number of "on" pixels by the total number of pixels for each preprocessed 2-dimensional (2-D) slice. Fractal dimension was calculated using the Hausdorff box-counting method in Matlab (MathWorks, Natick, Massachusetts).[48-50]

Image Processing

Z Stack images of fibrin matrices were visualized and quantified using multiple feature detection techniques of the Image Processing Toolbox in MATLAB (MathWorks).[51] Geometrical tubular elements were identified utilizing the fibermetric function, which employed multiscale second-order local structures (a vesselness measure) of eigenvalues from an Hessian pixilated matrix to detect tubular structures.[52] This function was used to identify tubular structures and was also used to filter out areas of dense fibrin fiber overlap. A mean filter function was used to identify densely populated fiber areas within each original *z* stack slice. These 2 preprocessing techniques (Figure 1) were combined into a single preprocessed image and used in subsequent segmentation and image-processing methods. Specifically, houghpeaks (Hough transform) and houghlines (Hough line) functions were applied to generate Cartesian line segments through the center of tubular structures to detect fibrin fibers.[46,52,53] Overall, fibrin fiber overlap and fibrin fiber length were calculated after Hough line generation, while fiber matrix porosity and fractal dimension were computed from preprocessed 2-D slices prior to segmentation.

Statistical Analysis

One-way analysis of variance (ANOVA) with the Tukey HSD post hoc test was performed on the fibrin samples incubated with 0.0, 6.0, and 10.0 mmol/L glucose conditions to determine statistical significance in fibrin clot structure characteristics. Statistical analysis was performed using SAS 9.4[54] (SAS, Cary, North Carolina) at a 95% confidence interval.

Molecular Simulations

The amount of glucose adsorbed to fibrinogen molecules in plasma can be studied using various methods. In addition to in vitro methods, computational methods can be used to estimate adsorption using docking simulations and MD methods. Molecular docking is a powerful tool in structural molecular biology and computer-assisted drug design. The goal of ligand–protein docking is to predict the predominant binding modes of a ligand with a known structure of the protein. Accurate docking methods search high-dimensional spaces effectively and use a scoring function that ranks candidate dockings.[55] Another powerful method that can be utilized is MD simulations, which are widely used in multiple disciplines of modern science and engineering.

To perform docking studies, glucose molecules (α-D-glucose) were docked onto a molecular fibrinogen model (3GHG[56] Figure 2A).[55] Initially, the docking simulations provided a maximum of 20 possible glucose–fibrinogen binding configurations. Since the fibrinogen molecule is large (340 kDa, 46 nm in length), this would have been an inefficient process. Thus, the fibrinogen molecule was divided into 10 longitudinal imaginary sections, and docking was performed on every section. The docking simulations were heuristic in nature, and hence the results were slightly different after each run. To select the best outcomes, we performed 5 sets of docking simulations for each section and selected the top best possible outcomes based on docking scores.

Molecular Dynamics Study

The molecular model of fibrinogen (3GHG[56] Figure 2A) was solvated using water in a periodic box with a volume 13.6 × 12.1 × 51.2 nm. Two concentrations of glucose were considered for this study. A glucose concentration of 10.23 mg/mL (similar to physiological conditions) was taken as the baseline case and also an increased level of glucose with 73 mg/mL was considered to

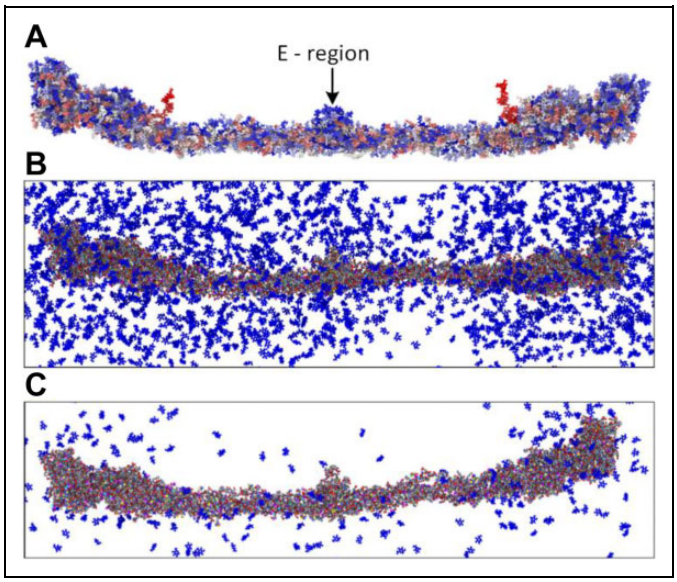

Figure 2. (A) Molecular model of fibrinogen (PDB code: 3GHG). (B) Fibrinogen and glucose in water at 73 mg/mL, and (C) 10 mg/mL glucose concentration (water molecules are hidden for clarity).

Table 1. Fibrin Clot Structure Parameter Outputs Under the 3 Glucose Conditions.

Parameter	0.0 mmol/L	6.0 mmol/L	10.0 mmol/L
N	843	857	643
Fibrin fiber overlap, average	14.67	14.29	10.33
Fibrin fiber overlap, standard deviation	4.85	2.33	2.31
Length, average, μm	24.96	24.31	22.88
Length, standard deviation, μm	1.77	0.89	1.04
Porosity, average, %	75.57	77.10	86.37
Porosity, standard deviation, %	4.94	3.81	3.68
Fractal dimension, average	1.754	1.736	1.632
Fractal dimension, standard deviation	0.039	0.037	0.055

study hyperglycemic effects. The molecular models of both high and low glucose concentration systems are shown in Figure 2B and C, respectively. The system was initially energetically minimized for 5000 steps, and this was followed by an equilibration for 50000 steps. For the production runs, a time step of 1 femtoseconds was used for time integration, and the simulation was carried out for 7 000 000 steps (7 nanoseconds). Using a Langevin thermostat, the temperature of the system was maintained at 310 K. The solvated models were created using visual MD (VMD), and the MD simulations were performed using Nanoscale Molecular Dynamics.[57]

Results

The protocols and imaging algorithms were used to quantify the effects of glucose concentration on fibrin clot structure and to evaluate differences in fibrin clot characteristics (fibrin fiber overlap, fibrin fiber length, fibrin matrix porosity, and fractal dimension). The number of samples (N), means, and standard deviations (SDs) for the fibrin clot structure characteristics (Table 1) were used to determine effects of glucose concentration on fibrin clot structure.

Representative images for the 3 glucose concentrations (Figure 3) illustrate variations in fibrin fiber structure characteristics and were used as a reference when discussing the characteristic difference. The 0.0 mmol/L glucose condition, while not physiologically relevant, provided a baseline comparison to the other glucose conditions.

Fibrin Fiber Overlap Variation With Glucose Concentration

The 0.0 mmol/L condition resulted in the highest fibrin fiber overlap average (14.67), and this value decreased as glucose concentration increased (Figure 4A). While this trend was also observed as glucose concentration increased from 0.0 to 6.0 mmol/L (14.29), the fibrin fiber overlap between the 0.0 and 6.0 mmol/L glucose conditions displayed no differences. However, fibrin fiber overlap for the 0.0 and 6.0 mmol/L glucose conditions was found to be higher ($P < .0001$) than for the 10.0 mmol/L condition (10.33).

Fibrin Fiber Length Variation With Glucose Concentration

Algorithms were used to determine longitudinal variations in Hough lines and to compute changes in fibrin fiber length. The 0.0 mmol/L condition (24.96 μm) resulted in the highest average fibrin fiber length (Figure 4B) and decreased as glucose concentration increased. Fibrin fiber length also decreased from the 6.0 mmol/L (24.31 μm) to 10.0 mmol/L condition (22.88 μm), and 1-way ANOVA was used to determine differences ($P < .0001$) between all 3 glucose concentrations at the selected 95% confidence interval.

Fibrin Matrix Porosity Variation With Glucose Concentration

Fibrin matrix porosity (Figure 4C) increased as glucose concentration increased. With the highest porosity observation in the 10.0 mmol/L glucose condition (86.37%), fibrin matrix porosity decreased for the 6.0 mmol/L condition (76.10%) and had the lowest porosity average in the 0.0 mmol/L condition (75.57%).

Fractal Dimension Variation With Glucose Concentration

Fractal dimension (Figure 4D) decreased as glucose concentration increased. With the lowest fractal dimension observed for the 10.0 mmol/L glucose condition (1.632), fractal dimension increased for the 6.0 mmol/L condition (1.736), and the highest fractal dimension was observed for the 0.0 mmol/L condition (1.754). One-way ANOVA was used to determine the fractal dimension for the 0.0 and 6.0 mmol/L glucose conditions, and

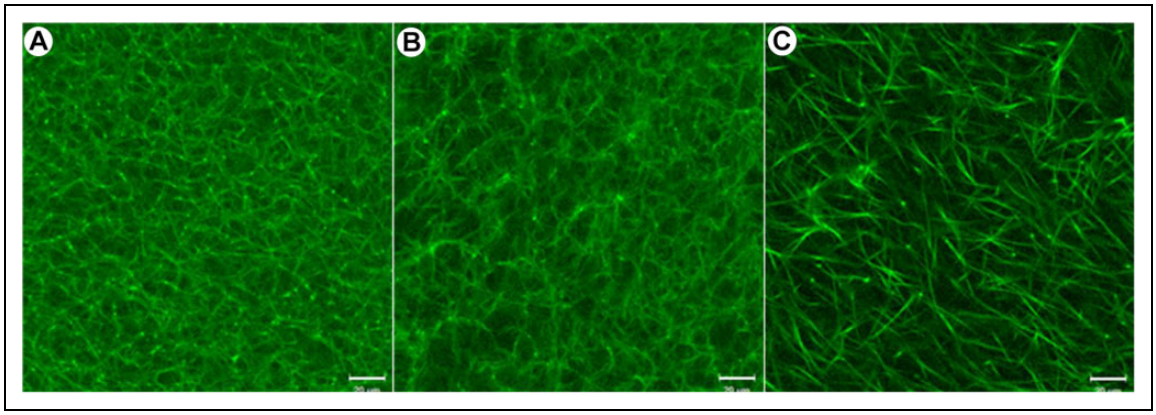

Figure 3. Representative fluorescence images of glycated fibrin clots at (A) 0.0 (B) 6.0, and (C) 10.0 mmol/L conditions.

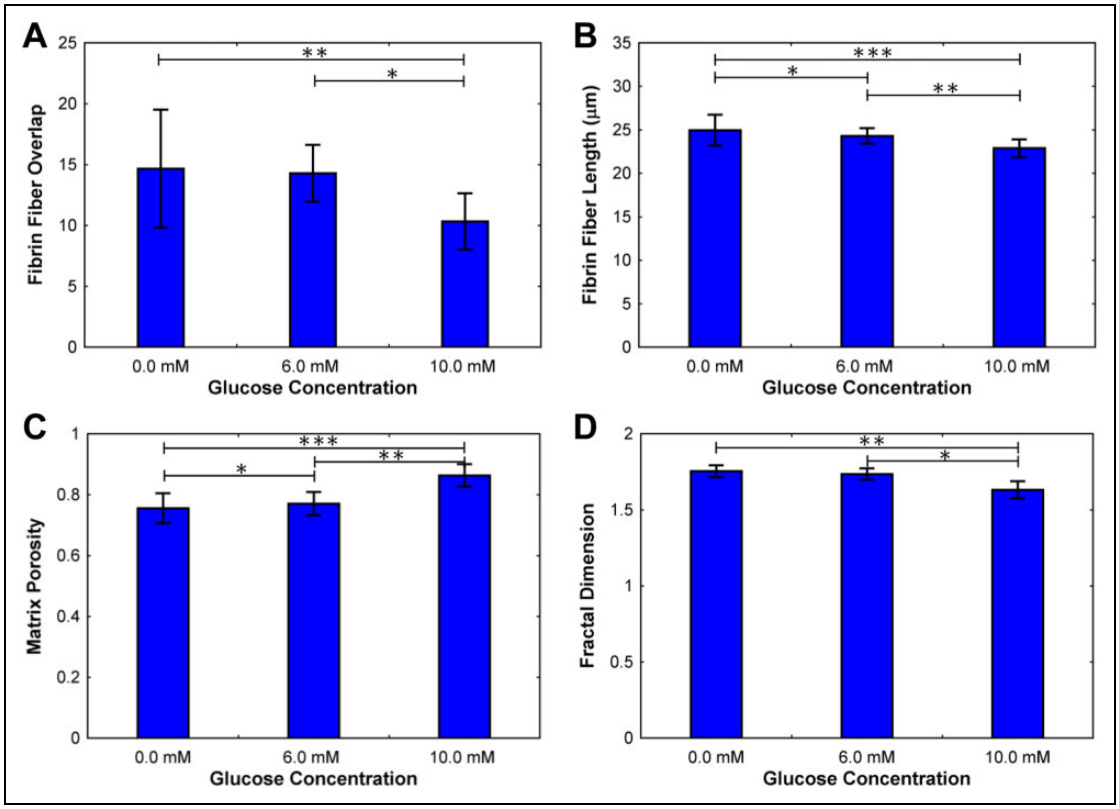

Figure 4. (A) Fibrin fiber overlap, (B) fibrin fiber length, (C) fibrin matrix porosity, and (D) fractal dimension for the 0.0, 6.0, and 10.0 mmol/L glucose incubation concentrations. Statistical significance: *$P < .0001$, **$P < .0001$, ***$P < .0001$ for samples with 0.0 mmol/L (N = 843), 6.0 mmol/L (N = 857), and 10.0 mmol/L (N = 643).

no differences were observed; however, for these cases, the fractal dimension was higher ($P < .0001$) compared to what was observed for the 10.0 mmol/L glucose condition.

Fibrinogen Glycation Independent of Fibrinogen Concentration

The colorimetric glucose assay employed an end point absorbance reading to evaluate the effect of glucose concentration on fibrinogen glycation. Fibrinogen glycation is suspected to influence changes in fibrin clot characteristics and promote macrovascular disease, but quantification of fibrinogen glycation under a constant fibrinogen concentration in vitro was novel to this experimentation. A standard curve (Figure 5) from known stock concentrations of diluted glucose standards was used as a comparison to calculate free glucose in samples of glucose conditions.

After 48 hours of incubation, free glucose concentration decreased in all 3 glucose conditions. The change in free glucose was used to calculate fibrinogen glycation over 48 hours of incubation at 37°C. For the 10.0 mmol/L condition,

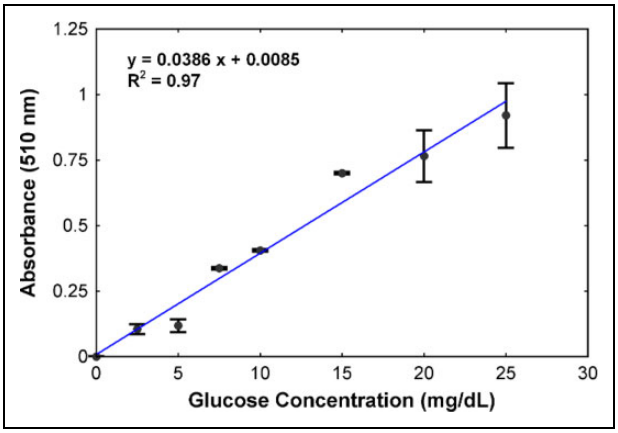

Figure 5. Standard curve from colorimetric glucose assay. The curve was developed by plotting the measured absorbance at 510 nm after 10 minutes of incubation versus concentration of glucose.

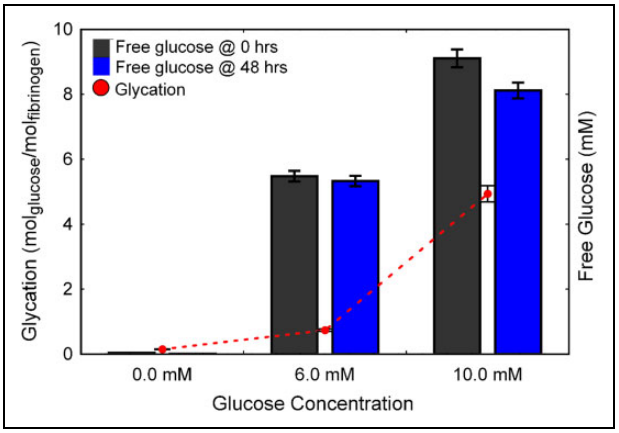

Figure 6. Change in free glucose and fibrinogen glycation after 48 hours of incubation at 37°C for each of the 3 glucose conditions.

Table 2. Colorimetric Glucose Assay Measurements Used to Quantify Fibrinogen Glycation After 48-Hour Incubation.

Variables	0.0 mmol/L	6.0 mmol/L	10.0 mmol/L
Free glucose @ $t = 0$, mmol/L	0.0424	5.476	9.104
Free glucose @ $t = 0$ standard deviation	0.049	0.122	0.200
Free glucose @ $t = 48$, mmol/L	0.012	5.328	8.116
Free glucose @ $t = 0$ standard deviation	0.059	0.347	0.431
Change in free glucose, mmol/L	0.031	0.149	0.989
Fibrinogen concentration, mmol/L	0.200	0.200	0.200
Glycation, $mol_{glucose}/mol_{fibrinogen}$	0.154	0.743	4.942
Glycation, standard deviation	0.011	0.047	0.063

4.942 $mol_{glucose}/mol_{fibrinogen}$ was the highest value of glycated fibrinogen that was measured (Table 2), and the trend revealed that glycated fibrinogen decreased with decreasing glucose concentration.

Although the initial absorbance readings showed a linear function of glucose concentration, the 48-hour readings did not. Therefore, fibrinogen glycation measurement over 48 hours was also not a linear function of initial glucose concentration. For the 6.0 mmol/L condition, 0.743 $mol_{glucose}/mol_{fibrinogen}$ was measured, and for the 0.0 mmol/L condition, 0.154 $mol_{glucose}/mol_{fibrinogen}$ was measured. Initial free glucose ($t = 0$), free glucose after 48 hours ($t = 48$), and glycated fibrinogen (Figure 6) were calculated from 15 sample trials per condition, and 1-way ANOVA was used to determine that fibrinogen glycation increased with increasing glucose concentration ($P < .0001$).

Molecular Docking Simulations

The results of the docking simulations are shown in Figure 7. The docking scores ranged from −4 to −5.2, with a maximum SD of 0.9. For every section out of 10 in the system, the top 5 configurations with minimum docking score was selected for further analysis (minimum score indicates better binding probability). The simulations were performed using Autodock Vina[55] as an extension to VMD.[58] Figure 7A shows the molecular model of fibrinogen used for the docking study, Figure 7B shows the glucose molecules attached to the fibrinogen molecule, and Figure 7C shows the glucose binding residues of the fibrinogen. The number of hydrogen bonds (H-bonds) formed by these glucose molecules with fibrinogen was identified and is displayed in Figure 7D. A total of 477 H-bonds were found between glucose and fibrinogen (within 3.5Å distance). The top 3 binding residues were identified as aspartic acid, glycine, and lysine.

In general, docking simulations are based on approximate scoring functions to predict the binding energy of a ligand and a protein complex, which are based on the hydrophobic information of the residues, empirical information of binding entities, and force fields. In this context, MD simulations can provide additional insights, in the presence of solvent, and more accurate binding based on force fields.[59]

Molecular Dynamics Simulation

The results of the 7-nanoseconds MD simulation were analyzed for adsorption of glucose on to fibrinogen. For the high-concentration glucose case, the number of glucose molecules forming strong H-bonds (2.5Å) were 67 and weak H-bonds (3.5Å) were 89 with the fibrinogen molecule. These adsorbed molecules are shown in Figure 8C and D for high and low glucose concentrations, respectively. The calculation provides an adsorption value of 67 $mol_{glucose}/mol_{fibrinogen}$ for the high-concentration case and 24 $mol_{glucose}/mol_{fibrinogen}$ for the low-concentration case. In a normal physiological fibrinogen concentration of 1.5 to 4 g/L, these glucose adsorption values become 0.05 to 0.142 mg/mL for the strong H-bond case and 0.07 to 0.188 mg/mL for weak H-bond case. A schematic of glucose attaching to the D-region of the fibrinogen molecule is shown in Figure 8A, and the formation of the H-bonds are shown in Figure 8B. For the low-glucose concentration case, the number of glucose molecules attaching to fibrinogen was

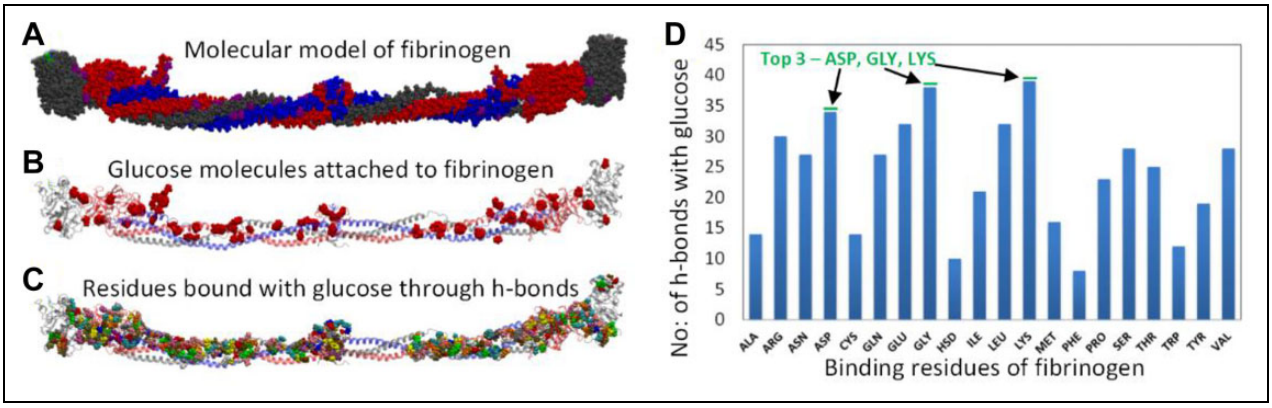

Figure 7. Molecular docking of glucose onto fibrinogen molecule. A, Molecular model of fibrinogen. B, Glucose molecules attached to fibrinogen (red and grain-like; fibrinogen molecule shown as transparent ribbon-like structure for reference). C, All residues that form hydrogen bonds with glucose molecules were identified. (D) The total number of H-bonds formed by each residue with glucose molecules is listed, with top residues identified as lysine, glycine, and aspartic acid.

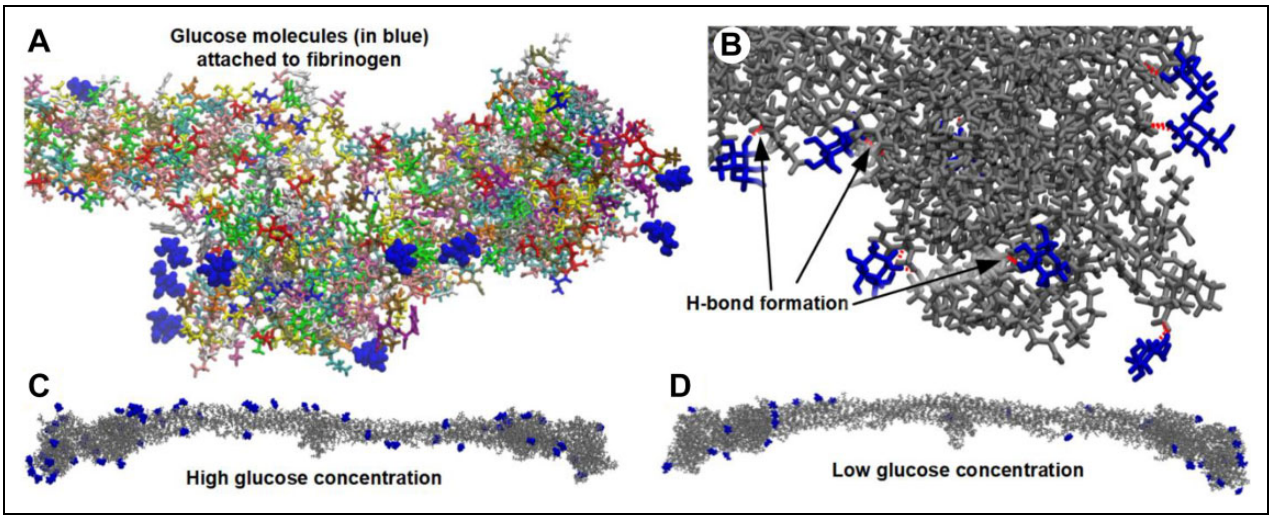

Figure 8. Molecular dynamics results of glucose adsorption to fibrinogen. (A) A close-up view of the attached glucose molecules near the fibrinogen molecule. (B) Glucose molecules adsorbed to fibrinogen with strong H-bonds. Glucose molecules that make strong H-bonds (within 2.5Å) with fibrinogen for both (C) high glucose concentration and (D) low glucose concentration.

tracked over time, and the results are displayed in Figure 9A. The graph shows the number of glucose molecules attaching within the distance ranging from 2.1Å to 2.9Å, which is the case for strong H-bond formation. The 2.1Å results (Figure 9A, lower curve) indicate that in the low-glucose concentration case (physiological), adsorption value is on average 24 molecules of glucose per fibrinogen molecule.

The number of H-bonds created by the host amino acid residues with glucose molecules is estimated and shown in Figure 9B for strong and weak cases. Unlike docking studies, MD simulations predict the top glucose bonding residues as arginine, asparagine, and lysine. We investigated further to understand more about glucose adsorption and attachment with the fibrinogen molecule. The hydropathy index (hydrophobicity vs hydrophilicity) of various residues was obtained from the literature[60] and plotted in Figure 9C. The number of H-bonds created and the percentage composition of various amino acids of fibrinogen are also shown in Figure 9C. Normally, hydropathy values are positive for hydrophobic and negative for hydrophilic. But for visual aid, the values were flipped (multiplied by −1), and the results are displayed in Figure 9C. This indicates that higher values of hydropathy demonstrate highly hydrophilic residues and vice versa. All values were normalized by dividing with 5, and our results indicate that the number of H-bonds formed is predominantly due to the hydrophilic nature of the residues and also the percentage composition. Although some residues are not strongly hydrophilic, such as serine and glycine, due to their high percentage composition, they tend to adsorb more glucose molecules.

Discussion

This study had 2 main aims. The first was to evaluate the effect of glucose concentration on fibrin clot characteristics at

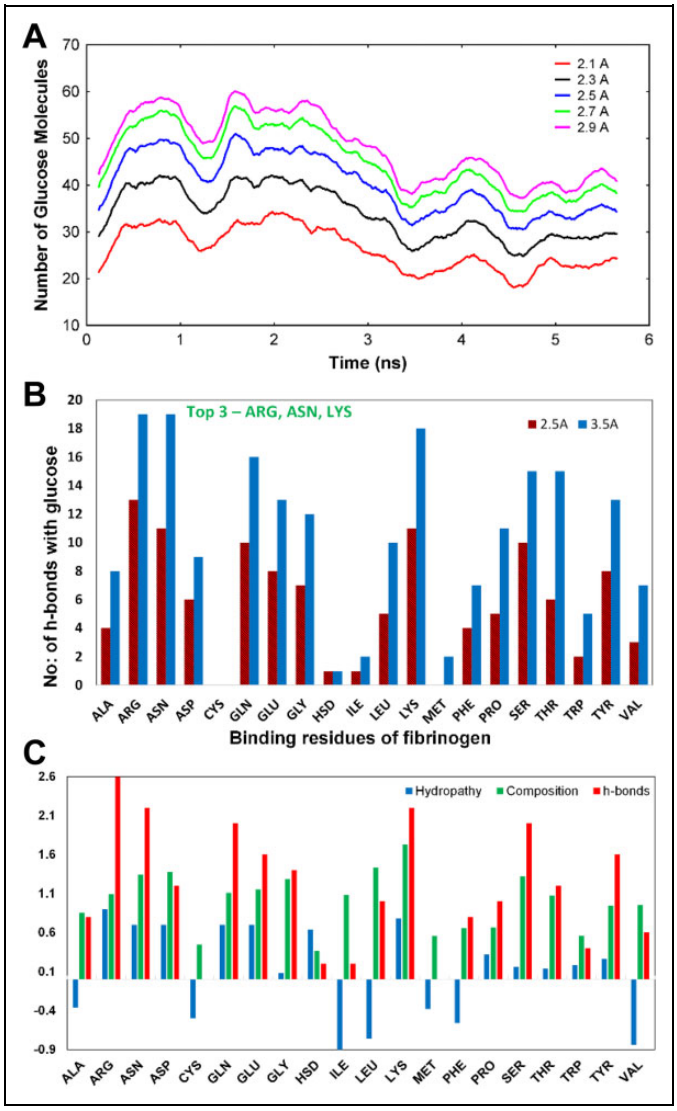

Figure 9. (A) Number of glucose molecules adsorbing to fibrinogen over time. The data were estimated with different bonding distances ranging from 2.1Å to 2.9Å, representing strong to weak H-bonding. (B) Number of H-bonds formed by glucose molecules with fibrinogen for the high glucose concentration case. Both strong and weak H-bonds formation was computed. (C) Analysis of H-bond formation of glucose with fibrinogen. Hydropathy (blue) of various residues, percentage composition (green) of residues on fibrinogen and the number of H-bonds (red) with glucose are shown. The vertical axis values should be multiplied by 5 to obtain actual values. The hydropathy values were flipped (multiplied with −1) to visually correlate with the H-bonds.

3 glucose concentrations. The second was to conduct fibrinogen glycation measurements, in a controlled fibrinogen system, and utilize molecular docking and dynamic simulations to justify how and why hyperglycemia increases fibrinogen glycation and alters clot characteristics.

First, the presented experimental methodology was used to visualize fibrin clot structure characteristics for the 3 glucose concentrations in a controlled in vitro fibrinogen system. The use of a 10% dyed fibrinogen concentration provided an effective balance of fluorescent and nonfluorescent fibrinogen. A higher percentage of total fibrinogen may have resulted in image saturation and the inability to distinguish fibrin fibers, and a lower dye percentage may have resulted in underdetection or indistinguishable variation in fibrin fiber characteristics. The selection of a 0.0 mmol/L glucose condition (although not physiologically relevant) provided a baseline comparison to the 6.0 and 10.0 mmol/L glucose conditions, and the effect of glucose concentration on the measured fibrin clot characteristics would not have been possible without a control for comparison. Additionally, the colorimetric glucose assay was used to measure changes in free glucose and to calculate fibrinogen glycation within the range of previously conducted in vivo studies.[20,31,61] Often, a glycated protein assay is used to measure glycated fibrinogen, but the colorimetric glucose assay was selected because (1) the glycated protein assay is not specific to fibrinogen and (2) fibrinogen is a large protein that adds additional accuracy concerns for protein digestion protocols. The glycated protein assay uses a generic protease to generate protein fragments prior to measuring glycation, and both irregular cleaving and the overall size of fibrinogen could explain the discrepancies between glycated fibrinogen of in vivo studies and the lower glycation measurements using this assay. Unfortunately, the colorimetric glucose assay is not possible in in vivo examination because fibrinogen is preexposed to glucose prior to measurement, and there is no baseline (0 hours) time point for comparison. Without more information on the exact binding site of glucose to fibrinogen, the glycated protein assay may be the best method to currently quantify glycated fibrinogen in vivo.

Second, the presented computational methodology was used to distinguish fibrin clot characteristics that were morphologically different in the 3 glucose conditions. Multiscale, second-order local structures were calculated, and this was found to be an effective preprocessing approach when coupled with a mean filter function. However, both functions were necessary to detect the local likelihood that a vessel was present for densely populated fiber areas and feature detection methods that were not considered for local geometry or accounted for highly populated local fibrin areas that may have resulted in less accurate recognition of tubular features. Overall, the ability of the presented computational methodology to detect fibrin matrix features over multiple size ranges may provide a methodology to inspire future in vivo experimentation of fibrin clot characteristics.

Fibrin fiber overlap was used as a quantitative reference to examine the connective behavior of detected fibrin fiber aggregates. Differences in fibrin fiber overlap were not observed between the 0.0 and 6.0 mmol/L glucose conditions, and this can be explained by differences in fiber length outputs for these conditions. Since the average fiber length in the 6.0 mmol/L glucose condition was less than in the 0.0 mmol/L condition, the shorter fibers were less likely to overlap with other randomly oriented shorter fibers in the 6.0 mmol/L condition. While another study has shown that glucose concentration increased fibrin fiber overlap, fibrin fiber overlap at glucose

concentrations higher than 10.0 mmol/L also decreased in this study. However, different computational methodologies and different macromolecule concentrations (thrombin, fibrinogen, and FXIII) were conducted in that experimental study, so the results may not be comparable.[46]

It is difficult to examine the true effect of glucose concentration on fibrin fiber length from LSM images (2-dimensional images of 3-dimensional structures); however, fibrin fiber length was measured to confirm that dehydration did not compromise the results. Although fibrin fiber length decreased with increasing glucose concentration, it is difficult to assess the true effects of glucose concentration on fibrin fiber length. However, it is promising that fibrin fiber length measurements are in agreement with fibrin fiber length averages (23 ± 9 μm) from previous studies and confirm dehydration did not affect results using the presented methodology.[62,63]

While fibrin matrix porosity calculated the fraction number of "on" pixels and would presume to be a measure of clot permeability, porosity measurements were actually an indication of fibrin fiber density. Samples were homogenized, and equal amounts of fibrinogen and thrombin were used to polymerize; higher porosity measurements are actually an indication of more densely compacted formed fibrin fibers. Many studies have presented the effect of protein glycation on fibrin fiber density, clot stability, resistance to lysis, and their influences of clotting risk, but none of these studies have examined the independent effect of glucose concentration on fibrin fiber density in a controlled in vitro fibrinogen system.[20,31-36,44,64] As hypercoagulable states such as DM present the risk to form more compact clots, increased fiber density provides further evidence that glucose concentration, via increased fibrinogen glycation, increases glycated clot resistance to fibrinolysis.

Measurement of fractal dimension (d_f) is becoming increasingly utilized as a potential biomarker to diagnose macrovascular risk because previous studies have demonstrated how changes in d_f relate to changes in clot mass.[48,65-67] From fibrin scanning electron microscopy studies, higher d_f is associated with a denser fibrin clot structure, but a reverse trend was observed with our LSM studies. Therefore, d_f measurements from confocal microscopy studies where a dye percentage is applied may better explain fibrin fiber density and clotting rate rather than changes in mass. Examining the relationship between thrombin concentration and d_f with constant fibrinogen concentration, Hawkins et al (2012)[68] found that clots imaged using confocal microscopy were qualitatively different in clot architecture, d_f increased with increasing thrombin concentration (ie, reaction rate) and were densest at the highest thrombin concentration.[69] Compared to our findings, this trend suggests increased glucose concentration actually slows clotting time as (1) the lowest d_f was measured for the 10.0 mmol/L glucose condition, (2) the 10.0 mmol/L condition produced the densest formed fibers (highest porosity reading), and (3) limited change in d_f and fibrinogen glycation was observed between the 0.0 mmol/L (1.754; 0.0308 $mol_{glucose}/mol_{fibrinogen}$) and 6.0 mmol/L (1.736; 0.743 $mol_{glucose}/mol_{fibrinogen}$) glucose conditions. Additionally, kinetic measurements of fibrinogen polymerization time indicate that the time to form a stable thrombus is significantly higher (6.6 vs 7.3 minutes, $P = .021$) in patients with diabetes, but these results were not conducted at a consistent fibrinogen concentration.[70] Additionally, contamination of hemostasis samples with a glucose-containing solution found diluting whole blood, with increasing glucose concentration ($P < .0001$) drastically prolonged clot formation time, which further supports our findings.[71] Although hyperglycemia is associated with enhanced thrombin formation, platelet activation, and resistance to lysis, in reality, it is likely that the combination of increased fibrinogen and thrombin concentrations, in addition to fibrinogen glycation, is what drives clot formation and causes a prolonged clotting time with densely formed fibrin fibers. Although not conducted in this study, a lower d_f from LSM data likely signifies thrombus formation that is more resistant to lysis and could be used to explain the increased clotting risk in the hypercoagulable state of DM with additional experimentation.

Conclusion

Algorithms coupled with statistical analysis were used to determine correlations between glucose concentration and fibrin clot structure characteristics. The results of this research support previous in vivo findings that hyperglycemia alters fibrin clot structure in patients with diabetes, independent of fibrinogen concentration. Fibrin fiber length measurements were consistent with previous conducted studies and confirmed that the native structure of imaged conditions was maintained. Matrix porosity results indicated that glucose concentration increased fibrin fiber density. Fractal dimension decreased with increasing glucose concentration supporting literature that suggests glucose concentration slows thrombus formation time. Thus, it can be concluded that increased fibrinogen and thrombin concentrations in DM accelerates fibrin clot formation and produces thrombi of increased fiber density. Fibrinogen glycation was found to be highest under the hyperglycemic condition (10.0 mmol/L) and had a pronounced effect with increased glucose concentration. To our knowledge, this is the first study to examine the effects of glucose concentration on fibrinogen glycation, independent of fibrinogen concentration using a colorimetric glucose assay. The molecular docking and MD simulations suggest that glucose adsorption on fibrinogen is highly dependent on the concentration of the glucose present in plasma. The docking results suggest a high affinity of glucose molecules to the hydrophobic amino acid residues. The MD results also indicate that the affinity is strongly governed by hydrophobicity, location of the amino acid on fibrinogen, and the percentage composition in the fibrinogen. Overall, imaging and glycation results support the notion that hyperglycemia increases fibrinogen glycation and changes morphological clot characteristics. As significant differences in clot structure characteristics were distinguishable, this technique could provide researchers, scientists, and medical professionals with an alternative diagnostic tool for

evaluation of clotting risk if adapted to human plasma and coupled with the appropriate epidemiological data.

Authors' Note

The content is solely the responsibility of the authors and does not necessarily represent the official views of the National Institutes of Health. Our institution does not require ethical approval for reporting individual cases or case series. Informed consent for patient information to be published in this article was not obtained because no patient data were used in this study.

Declaration of Conflicting Interests

The author(s) declared no potential conflicts of interest with respect to the research, authorship, and/or publication of this article.

Funding

The author(s) disclosed receipt of the following financial support for the research, authorship, and/or publication of this article: The research reported in this publication was supported by the National Heart, Lung, and Blood Institute of the National Institutes of Health under Award Number K01HL115486. This study was also supported in part by resources and technical expertise from the Georgia Advanced Computing Resource Center, a partnership between the University of Georgia Office of the Vice President for Research and Office of the Vice President for Information Technology.

ORCID iD

Sumith Yesudasan http://orcid.org/0000-0001-6379-2138
Rodney D. Averett http://orcid.org/0000-0001-8634-0599

Supplemental Material

Supplemental material for this article is available online.

References

1. Doolittle RF. Fibrinogen and fibrin. *Annu Rev Biochem*. 1984;53:195-229. doi:10.1146/annurev.bi.53.070184.001211.
2. Huang S, Mulvihill ER, Farrell DH, Chung DW, Davie EW. Biosynthesis of human fibrinogen. Subunit interactions and potential intermediates in the assembly. *J Biol Chem*. 1993;268(12):8919-8926.
3. Binnie CG, Lord ST. The fibrinogen sequences that interact with thrombin. *Blood*. 1993;81(12):3186-3192.
4. La Cilia, Corte AL, Philippou H, Ariëns RA. Role of fibrin structure in thrombosis and vascular disease. *Adv Protein Chem Struct Biol*. 2011;83:75-127. doi:10.1016/B978-0-12-381262-9.00003-3.
5. Fogelson AL, Keener JP. Toward an understanding of fibrin branching structure. *Phys Rev E Stat Nonlin Soft Matter Phys*. 2010;81(5 pt 1):051922. doi:10.1103/PhysRevE.81.051922.
6. Chernysh IN, Nagaswami C, Weisel JW. Visualization and identification of the structures formed during early stages of fibrin polymerization. *Blood*. 2011;117(17):4609-4614. doi:10.1182/blood-2010-07-297671.
7. Ryan EA, Mockros LF, Weisel JW, Lorand L. Structural origins of fibrin clot rheology. *Biophys J*. 1999;77(5):2813-2826. doi:10.1016/S0006-3495(99)77113-4.
8. Hantgan RR, Hermans J. Assembly of fibrin. A light scattering study. *J Biol Chem*. 1979;254(22):11272-11281.
9. Lord ST. Molecular mechanisms affecting fibrin structure and stability. *Arterioscler Thromb Vasc Biol*. 2011;31(3):494-499. doi:10.1161/ATVBAHA.110.213389.
10. Weisel JW. Structure of fibrin: impact on clot stability. *J Thromb Haemost*. 2007;(5 suppl 1):116-124. doi:10.1111/j.1538-7836.2007.02504.x.
11. Carr ME. Diabetes mellitus: a hypercoagulable state. *J Diabetes Complications*. 2001;15(1):44-54.
12. Osende JI, Badimon JJ, Fuster V, et al. Blood thrombogenicity in type 2 diabetes mellitus patients is associated with glycemic control. *J Am Coll Cardiol*. 2001;38(5):1307-1312.
13. American Diabetes A. Diagnosis and classification of diabetes mellitus. *Diabetes Care*. 2009;32(suppl 1):S62-S67. doi:10.2337/dc09-S062.
14. Nieuwdorp M, Stroes ES, Meijers JC, Büller H. Hypercoagulability in the metabolic syndrome. *Curr Opin Pharmacol*. 2005;5(2):155-159. doi:10.1016/j.coph.2004.10.003.
15. Lemkes BA, Hermanides J, Devries JH, Holleman F, Meijers JC, Hoekstra JB. Hyperglycemia: a prothrombotic factor? *J Thromb Haemost*. 2010;8(8):1663-1669. doi:10.1111/j.1538-7836.2010.03910.x.
16. Grant PJ. Diabetes mellitus as a prothrombotic condition. *J Intern Med*. 2007;262(2):157-172. doi:10.1111/j.1365-2796.2007.01824.x.
17. Ceriello A. Coagulation activation in diabetes mellitus: the role of hyperglycaemia and therapeutic prospects. *Diabetologia*. 1993;36(11):1119-1125.
18. Centers for Disease Control and Prevention. Long-term Trends in Diabetes. 2017; https://www.cdc.gov/diabetes/statistics/slides/long_term_trends.pdf. Accessed April 19, 2018.
19. Fonseca D, Gilberto S, Ribeiro-Silva C, et al. The role of fibrinogen glycation in ATTR: evidence for chaperone activity loss in disease. *Biochem J*. 2016;473(14):2225-2237. doi:10.1042/BCJ20160290.
20. Pieters M, van Zyl DG, Rheeder P, et al. Glycation of fibrinogen in uncontrolled diabetic patients and the effects of glycaemic control on fibrinogen glycation. *Thromb Res*. 2007;120(3):439-446. doi:10.1016/j.thromres.2006.10.016.
21. Dobesh PP. Economic burden of venous thromboembolism in hospitalized patients. *Pharmacotherapy*. 2009;29(8):943-953. doi:10.1592/phco.29.8.943.
22. Engelgau MM, Geiss LS, Saaddine JB, et al. The evolving diabetes burden in the United States. *Ann Intern Med*. 2004;140(11):945-950.
23. Grundy SM, Benjamin IJ, Burke GL, et al. Diabetes and cardiovascular disease: a statement for healthcare professionals from the American Heart Association. *Circulation*. 1999;100(10):1134-1146.
24. Scott RA, Freitag DF, Li L, et al. A genomic approach to therapeutic target validation identifies a glucose-lowering GLP1R variant protective for coronary heart disease. *Sci Transl Med*. 2016;8(341):341ra76 doi:10.1126/scitranslmed.aad3744.
25. Barazzoni R, Zanetti M, Davanzo G, et al. Increased fibrinogen production in type 2 diabetic patients without detectable vascular

complications: correlation with plasma glucagon concentrations. *J Clin Endocrinol Metab*. 2000;85(9):3121-3125. doi:10.1210/jc.85.9.3121.
26. Bruno G, Cavallo-Perin P, Bargero G, Borra M, D'Errico N, Pagano G. Association of fibrinogen with glycemic control and albumin excretion rate in patients with non-insulin-dependent diabetes mellitus. *Ann Intern Med*. 1996;125(8):653-657.
27. Mayne EE, Bridges JM, Weaver JA. Platelet adhesiveness, plasma fibrinogen and factor-Viii levels in diabetes mellitus. *Diabetologia*. 1970;6(4):436-440. doi:10.1007/Bf01212078.
28. Le DS, Miles R, Savage PJ, et al. The association of plasma fibrinogen concentration with diabetic microvascular complications in young adults with early-onset of type 2 diabetes. *Diabetes Res Clin Pract*. 2008;82(3):317-323. doi:10.1016/j.diabres.2008.08.019.
29. Stec JJ, Silbershatz H, Tofler GH, et al. Association of fibrinogen with cardiovascular risk factors and cardiovascular disease in the Framingham Offspring Population. *Circulation*. 2000;102(14):1634-1638.
30. Machlus KR, Cardenas JC, Church FC, Wolberg AS. Causal relationship between hyperfibrinogenemia, thrombosis, and resistance to thrombolysis in mice. *Blood*. 2011;117(18):4953-4963. doi:10.1182/blood-2010-11-316885.
31. Dunn EJ, Ariëns RA, Grant PJ. The influence of type 2 diabetes on fibrin structure and function. *Diabetologia*. 2005;48(6):1198-1206. doi:10.1007/s00125-005-1742-2.
32. Dunn EJ, Philippou H, Ariëns RA, Grant PJ. Molecular mechanisms involved in the resistance of fibrin to clot lysis by plasmin in subjects with type 2 diabetes mellitus. *Diabetologia*. 2006;49(5):1071-1080. doi:10.1007/s00125-006-0197-4.
33. Collet JP, Park D, Lesty C, et al. Influence of fibrin network conformation and fibrin fiber diameter on fibrinolysis speed: dynamic and structural approaches by confocal microscopy. *Arterioscler Thromb Vasc Biol*. 2000;20(5):1354-1361.
34. Weisel JW. Fibrinogen and fibrin. *Adv Protein Chem*. 2005;70:247-299. doi:10.1016/S0065-3233(05)70008-5.
35. Weisel JW. The mechanical properties of fibrin for basic scientists and clinicians. *Biophys Chem*. 2004;112(2-3):267-276. doi:10.1016/j.bpc.2004.07.029.
36. Undas A, Ariëns RA. Fibrin clot structure and function: a role in the pathophysiology of arterial and venous thromboembolic diseases. *Arterioscler Thromb Vasc Biol*. 2011;31(12):e88-e99. doi:10.1161/ATVBAHA.111.230631.
37. Singh VP, Bali A, Singh N, Jaggi AS. Advanced glycation end products and diabetic complications. *Korean J Physiol Pharmacol*. 2014;18(1):1-14. doi:10.4196/kjpp.2014.18.1.1.
38. Gugliucci A, Menini T, Stahl AJC. Glycation of fibrinogen in diabetic patients: a practical colorimetric assay. *Glycosylation & Discase*. 1994;1(3):177-183.
39. Nawale RB, Mourya VK, Bhise SB. Non-enzymatic glycation of proteins: a cause for complications in diabetes. *Indian J Biochem Biophys*. 2006;43(6):337-344.
40. Adamczyk B, Struwe WB, Ercan A, Nigrovic PA, Rudd PM. Characterization of fibrinogen glycosylation and its importance for serum/plasma *N*-glycome analysis. *J Proteome Res*. 2013;12(1):444-454. doi:10.1021/pr300813h.
41. Suzuki M, Minowa K, Tokita A, et al. Laboratory evaluation of blood plasma separation device in children. *Pediatr Int*. 2010;52(6):891-892. doi:10.1111/j.1442-200X.2010.03278.x.
42. Lutjens A, te Velde AA, vd Veen EA, vd Meer J. Glycosylation of human fibrinogen in vivo. *Diabetologia*. 1985;28(2):87-89.
43. Pieters M, Covic N, van der Westhuizen FH, et al. Glycaemic control improves fibrin network characteristics in type 2 diabetes—a purified fibrinogen model. *Thromb Haemost*. 2008;99(4):691-700. doi:10.1160/TH07-11-0699.
44. Bembde AS. A study of plasma fibrinogen level in type-2 diabetes mellitus and its relation to glycemic control. *Indian J Hematol Blood Transfus*. 2012;28(2):105-108. doi:10.1007/s12288-011-0116-9.
45. Fan NK, Keegan PM, Platt MO, Averett RD. Experimental and imaging techniques for examining fibrin clot structures in normal and diseased states. *J Vis Exp*. 2015;(98):e52019. doi:10.3791/52019.
46. Norton DG, Fan NK, Goudie MJ, Handa H, Platt MO, Averett RD. Computational imaging analysis of glycated fibrin gels reveals aggregated and anisotropic structures. *J Biomed Mater Res A*. 2017;105(8):2191-2198. doi:10.1002/jbm.a.36074.
47. Spasovski G, Vanholder R, Allolio B, et al. Clinical practice guideline on diagnosis and treatment of hyponatraemia. *Intensive Care Med*. 2014;40(3):320-331. doi:10.1007/s00134-014-3210-2.
48. Evans PA, Hawkins K, Morris RH, et al. Gel point and fractal microstructure of incipient blood clots are significant new markers of hemostasis for healthy and anticoagulated blood. *Blood*. 2010;116(17):3341-3346. doi:10.1182/blood-2010-02-269324.
49. Curtis DJ, Williams PR, Badiei N, et al. A study of microstructural templating in fibrin-thrombin gel networks by spectral and viscoelastic analysis. *Soft Matter*. 2013;9(19):4883-4889. doi:10.1039/c3sm50263e.
50. Weisel JW. "Ta panta rhei". *Blood*. 2010;116(17):3123-3124. doi:10.1182/blood-2010-07-294033.
51. Matlab, User's. *Guide* [*computer program*]. Natick, MA: Matlab, User's; 1992.
52. Frangi AF, Niessen WJ, Vincken KL, Viergever MA. Multiscale vessel enhancement filtering. *MICCAI*. 1998;1496:130-137.
53. Aggarwal N, Karl WC. Line detection in images through regularized Hough transform. *IEEE Trans Image Process*. 2006;15(3):582-591.
54. "SAS 9.4 for windows." [*computer program*]. Cary, NC: SAS 9.4 for windows; 2012.
55. Trott O, Olson AJ. AutoDock Vina: improving the speed and accuracy of docking with a new scoring function, efficient optimization, and multithreading. *J Comput Chem*. 2010;31(2):455-461.
56. Kollman JM, Pandi L, Sawaya MR, Riley M, Doolittle RF. Crystal structure of human fibrinogen. *Biochemistry*. 2009;48(18):3877-3886. doi:10.1021/bi802205g.
57. Phillips JC, Braun R, Wang W, et al. Scalable molecular dynamics with NAMD. *J Comput Chem*. 2005;26(16):1781-1802. doi:10.1002/jcc.20289.
58. Humphrey W, Dalke A, Schulten K. VMD: visual molecular dynamics. *J Mol Graph*. 1996;14(1):33-38, 27-38.

59. Kruschel D, Zagrovic B. Conformational averaging in structural biology: issues, challenges and computational solutions. *Mol Biosyst*. 2009;5(12):1606-1616. doi:10.1039/b917186j.
60. Kyte J, Doolittle RF. A simple method for displaying the hydropathic character of a protein. *J Mol Biol*. 1982;157(1):105-132.
61. da Costa G, Gomes RA, Guerreiro A, et al. Beyond genetic factors in familial amyloidotic polyneuropathy: protein glycation and the loss of fibrinogen's chaperone activity. *PLos One*. 2011;6(10):e24850. doi:ARTN e24850. 10.1371/journal.pone.0024850.
62. Collet JP, Shuman H, Ledger RE, Lee S, Weisel JW. The elasticity of an individual fibrin fiber in a clot. *Proc Natl Acad Sci U S A*. 2005;102(26):9133-9137. doi:10.1073/pnas.0504120102. http://www.pnas.org/content/102/26/9133.abstract. Accessed April 19, 2018.
63. Baradet TC, Haselgrove JC, Weisel JW. Three-dimensional reconstruction of fibrin clot networks from stereoscopic intermediate voltage electron microscope images and analysis of branching. *Biophys J*. 1995;68(4):1551-1560. doi:10.1016/S0006-3495(95)80327-9.
64. Li W, Sigley J, Pieters M, et al. Fibrin fiber stiffness is strongly affected by fiber diameter, but not by fibrinogen glycation. *Biophys J*. 2016;110(6):1400-1410. doi:10.1016/j.bpj.2016.02.021.
65. Curtis D, Brown MR, Hawkins K, et al. Rheometrical and molecular dynamics simulation studies of incipient clot formation in fibrin-thrombin gels: an activation limited aggregation approach. *J Non-Newtonian Fluid Mech*. 2011;166(16):932-938. doi:10.1016/j.jnnfm.2011.04.016.
66. Lawrence MJ, Sabra A, Thomas P, et al. Fractal dimension: a novel clot microstructure biomarker use in ST elevation myocardial infarction patients. *Atherosclerosis*. 2015;240(2):402-407. doi:10.1016/j.atherosclerosis.2015.04.012.
67. D'silva L, Alikhan R, Stanford S, et al. Defining the reference range for blood clot gel point and fractal dimension. *J Thromb Haemost*. 2015;13:538-538.
68. Hawkins K, Badiei N, Weisel J, et al. Fractal dimension: a biomarker for detecting acute thromboembolic disease. *Crit. Care*. 2012;16(Suppl 1):431.
69. Undas A, Wiek I, Stêpien E, Zmudka K, Tracz W. Hyperglycemia is associated with enhanced thrombin formation, platelet activation and fibrin clot resistance to lysis in patients with acute coronary syndrome. *Eur Heart J*. 2008;31(8):1590-1595.
70. Viswanathan GN, Marshall SM, Balasubramaniam K, Badimon JJ, Zaman AG. Differences in thrombus structure and kinetics in patients with type 2 diabetes mellitus after non ST elevation acute coronary syndrome. *Thromb Res*. 2014;133(5):880-885. doi:10.1016/j.thromres.2014.01.033.
71. Shin HJ, Na HS, Lee S, Lee GW, Do SH. The effect of hyperglycemia on blood coagulation: In vitro, observational healthy-volunteer study using rotational thromboelastometry (ROTEM). *Medicine (Baltimore)*. 2016;95(35):e4703. doi:ARTN e4703 10.1097/MD.0000000000004703.